

TIG WELDING SKILL EXTRACTION  
USING A MACHINE LEARNING ALGORITHM

by

Shelby Huff

A thesis submitted to the Graduate Council of  
Texas State University in partial fulfillment  
of the requirements for the degree of  
Master of Science with a Major in Engineering  
with a concentration in Manufacturing Engineering  
December 2017

Committee Members:

Heping Chen, Chair

Young Ju Lee

Jitendra Tate

Ravi Droopad

**COPYRIGHT**

by

Shelby Huff

2017

## **FAIR USE AND AUTHOR'S PERMISSION STATEMENT**

### **Fair Use**

This work is protected by the Copyright Laws of the United States (Public Law 94-553, section 107). Consistent with fair use as defined in the Copyright Laws, brief quotations from this material are allowed with proper acknowledgement. Use of this material for financial gain without the author's express written permission is not allowed.

### **Duplication Permission**

As the copyright holder of this work I, Shelby Huff, authorize duplication of this work, in whole or in part, for educational or scholarly purposes only.

## **DEDICATION**

I would like to dedicate my thesis to my family members and friends for the constant support and encouragement throughout my pursuit of a Master's degree.

## **ACKNOWLEDGEMENTS**

I would like to thank Dr. Heping Chen for the research opportunity under his mentorship for over three years. I feel very fortunate for his guidance and support throughout the development of this thesis. I would also like to thank him for the postgraduate summer school opportunity in Shenyang, China.

I would like to thank Dr. Young Ju Lee for his guidance in computer coding algorithms.

I would like to thank Dr. Jitendra Tate and Dr. Vishu Viswanathan for guidance throughout my postgraduate degree and for teaching me the basics of scientific research. I would also like to thank Dr. Stand McClellan and Dr. Ravi Droopad for their valuable insight during the thesis defense.

I want to thank Dr. Ray Cook, Jason Wagner, and Sarah Rivas for their help and supervision in the research laboratories.

I would like to thank the Graduate College at Texas State University for the Thesis Research Support Fellowship. The award was used to purchase vital equipment needed in this thesis experimentation.

## TABLE OF CONTENTS

	Page
ACKNOWLEDGEMENTS .....	v
LIST OF TABLES .....	viii
LIST OF FIGURES .....	ix
ABSTRACT .....	xi
CHAPTER	
I. INTRODUCTION .....	1
Background .....	1
Industrial Robots .....	1
Welding .....	5
Artificial Intelligence & Machine Learning .....	9
II. LITERATURE REVIEW .....	12
Neural Networks .....	12
Support Vector Machines .....	16
Gaussian Process Regression .....	16
Origination of Thesis .....	17
III. PROPOSED SOLUTION .....	20
Process Modeling .....	20
Gaussian Process Regression .....	22
IV. EXPERIMENTATION .....	26
Robotic TIG Welding Experiments .....	26
V. RESULTS .....	33
Training .....	33
Validation Results .....	36

VI. CONCLUSION.....	38
Contribution .....	38
Future Work .....	38
APPENDIX SECTION .....	40
Appendix B. Mean and Variance of Width for Training Experiments .....	40
Appendix B. Mean and Variance of Width for Training Experiments .....	45
Appendix C. Current & Width of Validation Experiments .....	50
Appendix D. Mean & Variance of Width for Validation Experiments .....	50
LITERATURE CITED .....	51

## LIST OF TABLES

Table	Page
1. Machine Learning Algorithms used to Model the Welding Process .....	18
2. Covariance Functions.....	33
3. Predicted Current and Error of Test Data Set .....	34
4. Predicted Current and Error of Validation Data Set .....	36



## LIST OF FIGURES

Figure	Page
1. Estimated Annual Worldwide Supply of Industrial Robots 2008-2016 and 2017*-2020* .....	2
2. Types of Industrial Robots.....	3
3. Estimated Annual Supply of Industrial Robots at Year-end by Industries Worldwide 2014-2016 .....	4
4. Types of Arc Welding.....	6
5. TIG Welding Process Diagram.....	8
6. Machine Learning Methods .....	10
7. Arc Welding Process Model for Predicting Welding Parameters .....	21
8. Gaussian Process Regression.....	22
9. Autonomous TIG Welding System.....	26
10. Aluminum Weld Coupons Before & After Grinding .....	27
11. Welding Machine & Input Parameters a) Norstar TIG Machine b) Torch Parameters c) AC balance .....	27
12. Robot Program Parameters .....	28
13. Experiment #4.....	29
14. Training Experiment Weld Coupons a) Experiments 1-10 b) Experiments 11-20 c) Experiments 21-30 d) Experiments 31-40 e) Experiments 41-50 .....	30
15. Shading in Microsoft Paint .....	31
16. Validation Experiments #1-5 .....	32
17. Test Current vs Predicted Current from Test Data .....	35

18. Prediction Error from Test Data .....	35
19. Test Current vs Predicted Current from Validation Data .....	37
20. Prediction Error from Validation Data .....	37

## **ABSTRACT**

Tungsten Inert Gas (TIG) welding is the superior arc welding process used in the manufacturing industry for high quality welds. Skilled welders are capable of monitoring a weld bead and dynamically adjusting the welding parameters (current, voltage, speed, etc.) to produce a desired weld bead quality (width, height, depth). A shortage of skilled workers and motivation for industrial automation has increased research in welding process control and optimization. We propose a Machine Learning algorithm to model the TIG welding process and extract human skill. First, an automated TIG welding system uses an industrial robot to conduct aluminum welding experiments. Controlled process parameters and resultant weld bead quality measurements are used to form a welding process dataset. A Gaussian Process Regression (GPR) algorithm is applied to model the relationship in the dataset inputs variables and output variables. For a desired weld bead thickness, the required adjustment in welding current, or welding skill, can be predicted to robustly control the process. The addition of artificial intelligence to industrial robots can solve many automation solutions in the manufacturing industry dealing with complex processes.

## **I. INTRODUCTION**

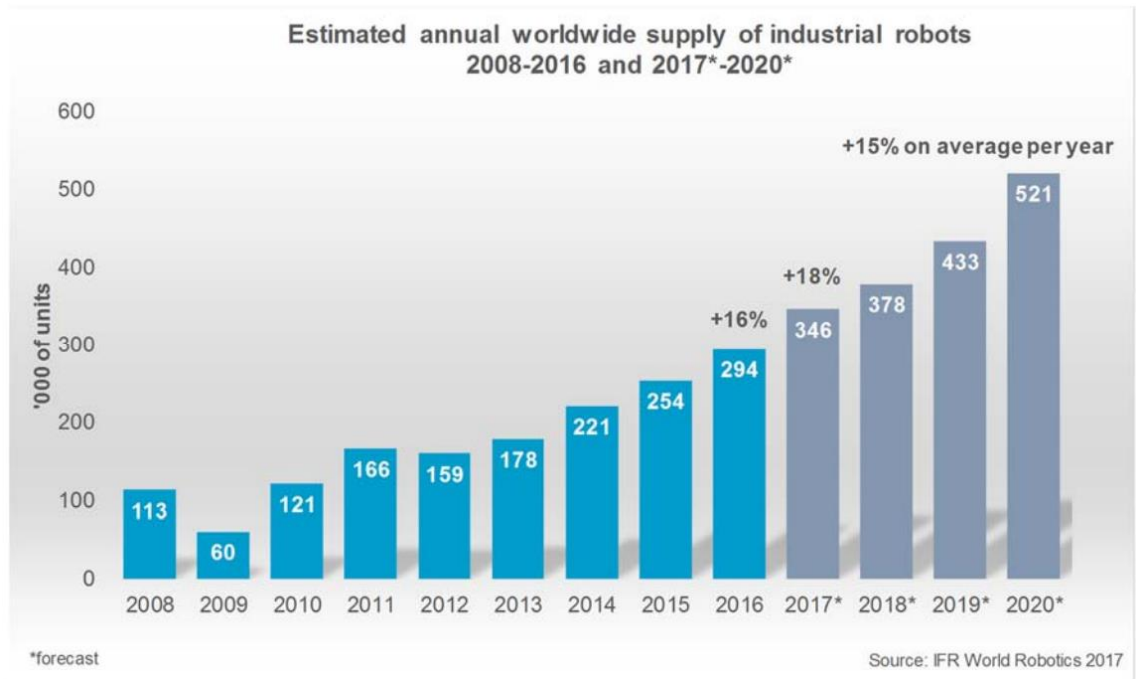
### Background

Arc welding is the process of joining two or more metals together using electrical energy. The two metals are heated by an electric arc and the atoms are fuse together. Upon cooling, the metals coalesce into one piece that is as strong as the original material strength. Arc welding is an essential process widely used in the manufacturing industry. However, the decreasing workforce of skilled workers has significantly hindered manufacturer's ability to utilize the welding process. Certification for a professional welder usually requires technical school instruction and can take several months. In response, engineers have chosen to use industrial robots to replace the human worker and increase productivity. Robot automation poses many advantages for simple processes; however, these machines struggle to automate dynamic processes. Researchers have attempted to overcome these limitations by equipping robots with artificial intelligence. Machine learning algorithms enable robots to sense dynamic environments and make intelligent changes like a human. The engineering challenge of this dissertation is to automate the welding process using an industrial robot and extract human skill using a machine learning algorithm.

### Industrial Robots


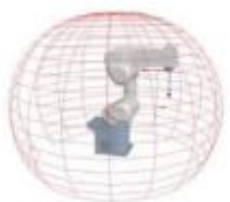




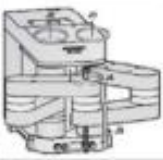








An increase in technology and computing power in the last few decades led to the use of industrial robots in the manufacturing industry. In 1961, the first prototype industrial robot was produced by GM by combining three key technology waves: the invention of Numerically Controlled Machines, popularity of the computer, and the creation of integrated circuits (Wallen, 2008). Industrial robot development increased

throughout the 70's and 80's but proved to be premature for the technology of that era. Since the global financial crisis of 2008, there has been dramatic increase in the use of industrial robots due to their advantages in automation. 2016 showed an increase of 16% to 294,312 units, a new peak for the fourth year in a row. The International Federation of Robotics (IFR) predicts an increase of 15% on average per year until 2020.



**Fig. 1 Estimated Annual Worldwide Supply of Industrial Robots  
2008-2016 and 2017\*-2020\*. Taken from ifr.org**

So, what is an industrial robot and why are they so beneficial? The International Organization for Standardization (ISO 8373:2012) defines them as “an automatically controlled, reprogrammable, multipurpose manipulator programmable in three or more axes, which can be either fixed in place or mobile for use in industrial automation applications.” There are many classes of industrial robots designed to meet the needs of different applications. A few of the most popular classifications include Cartesian, Parallel, SCARA, and Articulated robots.

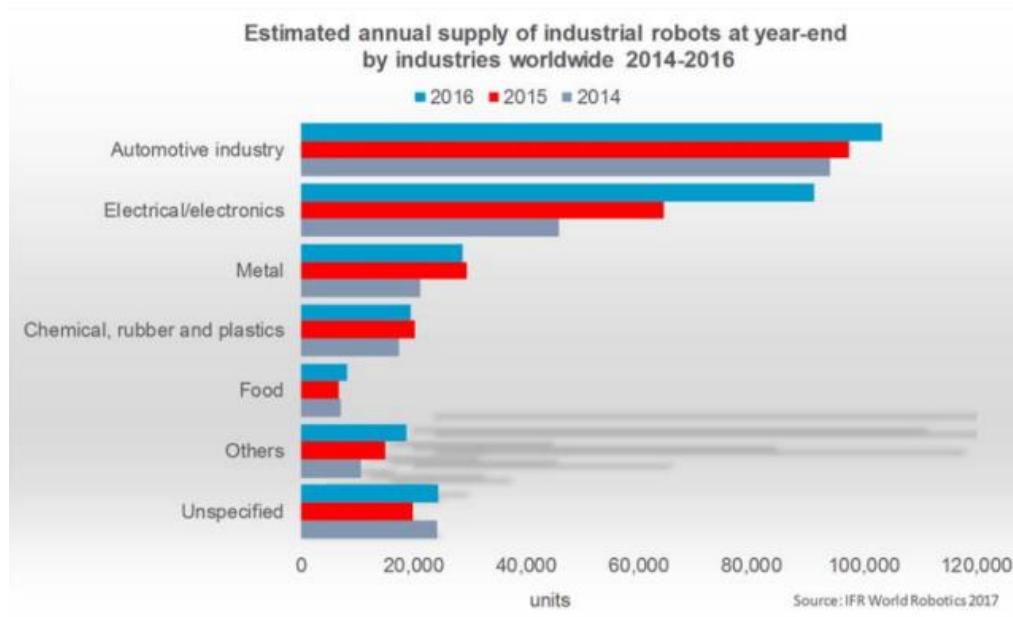
Principle	Kinematic Structure	Photo
<b>Articulated Robot</b> 		
<b>SCARA Robot</b> 		
<b>SCARA Robot</b> 		
<b>Cartesian Robot</b> 		
<b>Parallel Robot</b> 		

**Fig 2. Types of Industrial Robots. Taken from ifr.org**

Simpler-designed robots with only 4 axes and 4 degrees of freedom like the Cartesian and SCARA robot can be used for performing simpler manufacturing tasks, such as a pick and place or stamping operation. Articulated robots with 6 axes and 6 degrees of freedom are used for performing more complex manufacturing tasks, such as: welding, grinding, painting, assembly, palletizing, heavy material handling, and

packaging. The trend of manufacturers integrating automation in the last decade is due to the many benefits industrial robots possess including: high efficiency, high accuracy, high quality, 24/7 operational time, hazardous environment immunity, high payload, and reduced waste.

Of the 294,000 industrial robots used in the manufacturing industry worldwide, the focus of this dissertation is on welding robots. Welding robots are most popular in the Automotive and Metal industries.



**Fig. 3 Estimated Annual Supply of Industrial Robots at Year-end by Industries Worldwide 2014-2016. Taken from ifr.org**

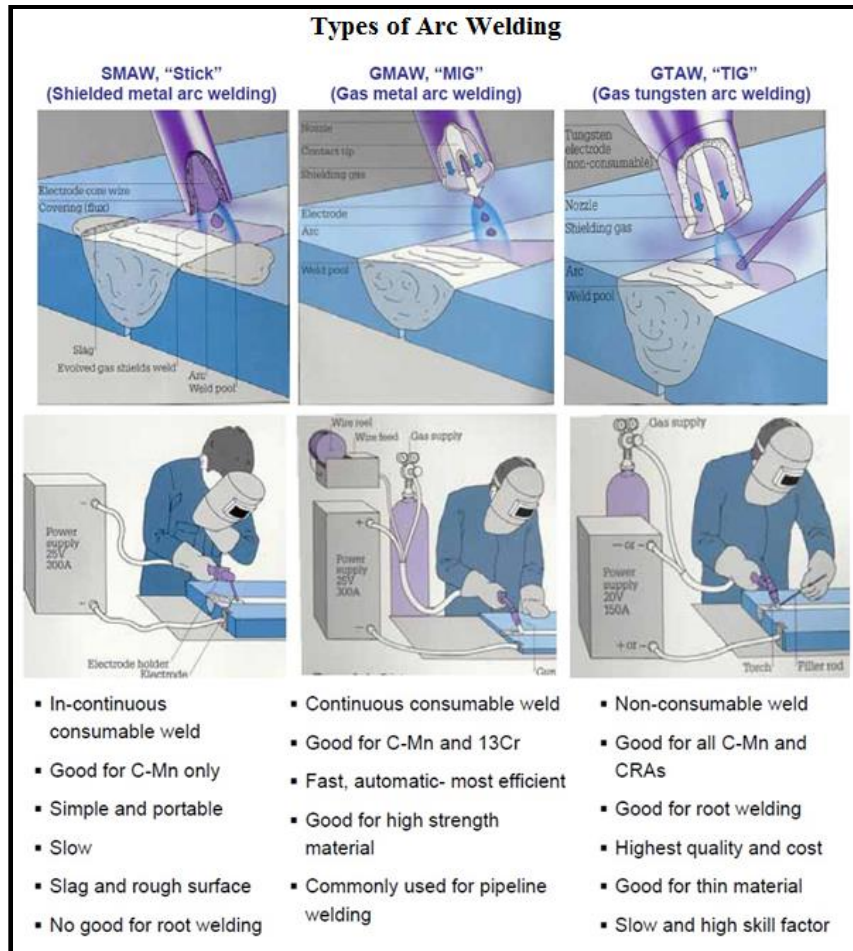
These two industries can account for 132,000 robots in 2016, which is 45% of the total supply. All manufacturers can purchase from the most popular industrial robot brands like Epson, Kawasaki, Fanuc, Kuka, and ABB. These robots can be easily programmed to automate a simple process; however, a “stock” industrial robot will struggle to produce consistent quality for dynamic processes under changing parameters,

noise, or uncertainties. An automated process failing on the manufacturing line will lower the throughput and demand human interaction. Intelligent decision-making systems with human-like capabilities are needed to increase industrial robot's flexibility. Researchers propose intelligent solutions by incorporating real time sensors and machine learning algorithms. Intelligence is vital in a manufacturing process like arc welding where the process parameters are changing and the system must deal with noise and uncertainties.

### Welding

Joining two metals together is a process needed extensively in the manufacturing industry. Arc welding is the most popular form of metal joining because the strength of a good quality weld joint is equal to the initial material strength. Skilled welders use different welding methods depending on the type of material, thickness of material, available power source, type of weld joint, working environment, and the quality of weld needed.





**Fig 4. Types of Arc Welding (Lee, 2007)**

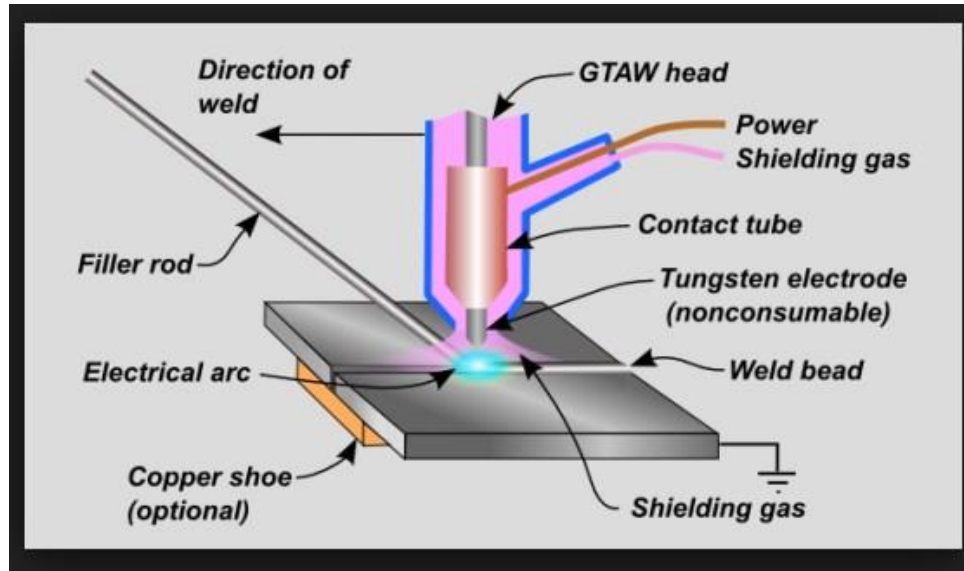
The most-classic form of arc welding is known as Shielded Metal Arc Welding (SMAW or "Stick"). An electric arc is struck between a consumable electrode and the workpiece. The consumable electrode is melted into the weld bead as the filler material and is coated in flux that acts as a shielding gas when burnt. This process is extremely reliable; however, Stick yields low quality weld beads, it is limited to ferrous materials, and it is rather slow.

The next form is known as Gas Metal Arc Welding (GMAW) or Metal Inert Gas (MIG). MIG welding consists of a continuous, consumable wire being fed into the weld as both the electrode and filler material. At the same time, the welding gun supplies a

protection gas to prevent weld bead contamination. The MIG process is easy to learn, the welding speeds are fast, and it yields good quality weld beads. However, MIG is limited to thick materials and mostly only ferrous metals. Also, welding parameters current and wire feed rate are constant and not designed to adjust during the welding process.

Lastly, Gas Tungsten Arc Welding (GTAW or “TIG”) is the most complex process of the three. A non-consumable electrode is used to strike an arc and heat the weld bead area while being protected by inert gas. During the process, the welding torch is moved at a given speed, torch angle, and distance from the workpiece. At the same time, consumable metal is fed into the weld bead area for reinforcement if it is needed. Concurrently, the current can be adjusted to control heat flow. The skill needed of a TIG welder to simultaneously control the current with a foot pedal, move the electrode torch with one hand, and add filler material with the opposite hand is what makes this method difficult to learn. Ironically, the dynamic control of the welding parameters is what welders prefer once the skill is mastered. TIG welding’s active-parameter control enables the welder to gain the most heat control of the weld pool compared to Stick or MIG. Consequently, TIG welding is the preferred arc welding process for thin metals, nonferrous metals, and most importantly when weld quality is important (Patel, 2014)

Manual TIG welding is a dynamic manufacturing process where the input welding parameters directly affect the output welding quality. There are many input welding parameters that the welder is responsible for setting and controlling: 1 Tungsten electrode material type and diameter, 2 ceramic gas cup size, 3 torch orientation angle, 4 torch travel speed, 5 arc distance, 6 inert gas type, 7 gas flow rate, 8 amount of current, 9 AC balance, etc.



**Fig 5. TIG Welding Process Diagram (Patel, 2014)**

A professional welder can generally preselect ideal parameter settings based off the material type, thickness, and desired weld quality. Once the welding arc is struck with the workpiece under the initial parameters, the welder actively monitors the dynamic weld pool and intelligently adjusts the welding parameters current, travel speed, and arc distance accordingly. A skilled welder's intelligent response can decrease inconsistency in weld bead quality. The weld bead quality can be measured by the 3d weld pool convexity, the weld bead width, depth of penetration, or mechanical strength. Given a desired weld bead quality, we attempt to extract human welder's parameter changing skill.

Automating a manufacturing process using an industrial robot, the system gains many advantages. An ABB robot is capable of repeating a programmed weld path with the accuracy of  $\pm 0.03\text{mm}$  and up to  $2.5\text{m/s}$  (ABB, 2017). Programmers use these advantages to simulate a virtually perfect human welder. First, we can move the welding torch at a constant speed. Second, we can program the welding torch at a constant torch

angle and constant arc distance. Third, we can control the amount of current discretely. Fourth, we can repeat the same weld path accurately each time. Once constant input parameters are established, one isolated input parameter can be adjusted. Finally, sensors can be used to measure and analyze the relationship between an isolated input parameter and the resultant weld bead quality.

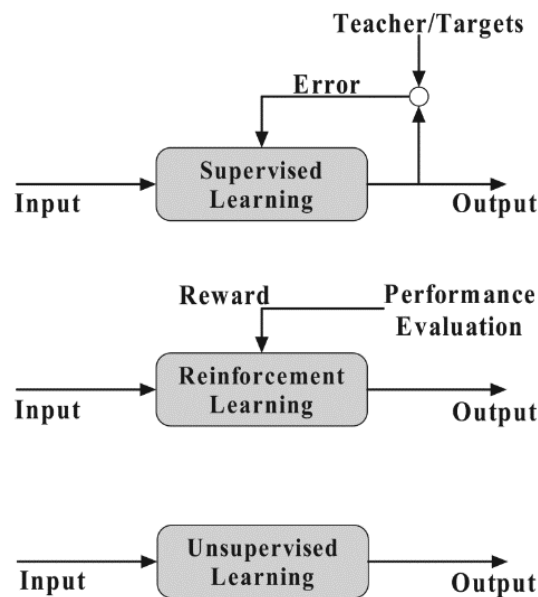
### Artificial Intelligence & Machine Learning

Artificial Intelligence is the science of “creating computer programs or machines capable of behavior we would regard as intelligent if exhibited by human.” Early computer science pioneers found success in the 50s 60s by creating computer vision algorithms and natural language recognition (Kaplan, 2016). However, progress was plagued by technology limitations. An increase in computational power and large data sets has revitalized AI development. An increase in AI use can be witnessed in everyday lives. For example, Google image searches or smartphone speech recognition are two basic technologies utilizing large datasets. More complex ideas being developed today include self-driving cars, humanoid robots, and intelligent healthcare systems.

Scientists seek to add intelligent abilities to a computer system through reasoning, knowledge, planning, learning, natural language processing, and perception (Russel, 1995). Intelligent capabilities can be used by machines to automatically solve complex problems. In order to solve a problem using a computer (or machine), we need an algorithm. According to Alpaydin (2014), “an algorithm is a sequence of instructions that should be carried out to transform the input to output.” The coupling of computer algorithms and large data sets has led to the development of machine learning algorithms. Machine Learning (ML) is the process of defining a process model, learning how to

optimize the parameters, and ultimately gain descriptive knowledge of a process or make predictions in the future. Optimization and predictability are two major attributes that can be utilized by industrial robots since companies are increasingly looking for automated solutions.

Taking a computer science tool that typically uses theoretical datasets and applying it to a practical manufacturing process can be challenging. For example: datasets can include many variable, relationships of inputs and outputs may be nonlinear, or there may exist noise and uncertainties. So, we can organize the different types of ML algorithms into taxonomy, based off the data structure of the respective process data:



**Fig 6. Machine Learning Methods (Wang, 2012)**

1) Supervised Learning – Given a dataset of inputs and outputs for a process, first divide the dataset into training data and test data. Then find a mapping between the inputs and outputs based on the training dataset. Then make predictions on the input of the test dataset, which has been never seen in the training process. Prediction performance can be

measured since the output of the training data is already given. Examples of supervised learning algorithm techniques include: ANOVA, DOE Taguchi, classification, regression, support vector machines, neural networks, and decision tree.

2) Unsupervised learning – Given a dataset of inputs and outputs for a process, extract patterns or relationships in the input data. Since this method is open looped, there is no feedback from the environment. Examples of unsupervised learning algorithm techniques include: self-organizing maps, clustering.

3) Reinforcement Learning – Given an online system, input and output data is produced through interaction with the environment. This approach learns a mapping through trial and error. So, every input action yields a feedback from the environment. The goal is to maximize the expected cumulative reward. Examples of reinforcement learning algorithm techniques include: temporal-difference, deep learning.

## II. LITERATURE REVIEW

### Neural Networks

Preliminary studies were done by W. Zhang & Y. Zhang (2012) to model the human welding process using a statistical technique called autoregressive with exogenous terms model, similar to “moving averages.” In this experimental setup, a laser camera-vision system is set up to sense the real time 3D weld pool surface of a human welder, TIG welding a steel pipe. The input to the model is the sensing of the 3D pool surface quality (weld pool length, width, and convexity). The output of the system is the changes the human welder makes to the welding parameters (speed, current, and arc distance). It was discovered that the linear model was insufficient to model a nonlinear welding process. However, key findings were made that many researchers used later: 1) A human welder makes adjustments on the welding parameters based on the real time and previous weld pool surface from approximately 1.5s to 3s previously. 2) A human welder also makes adjustments on the welding parameters based on the previous adjustments he has made 1s prior. These characteristics show the arc welding process is a nonlinear and time-delayed process.

Then, Wang & Liu teamed up with W. Zhang and Y. Zhang (2012) at the University of Kentucky and took a non-linear modeling approach to modeling the welding process, called least squares algorithm. The goal here was to predict weld bead penetration in the form of backside weld bead width. So, Wang et al. used the same TIG welding process and laser vision system as W. Zhang and Y. Zhang (2012), but modeled the data differently. The input parameters consisted of real time 3d weld pool surface quality (weld pool width, length, convexity). Output of the system was the backside

width of the resultant weld bead. The least square algorithm was capable of predicting the backside width with an acceptable variance of  $s^2=0.39 \text{ mm}^2$ . This proved that data could be extracted from the welding process to predict weld bead quality.

Further research at the University of Kentucky was conducted by Liu, W. Zhang, and Y. Zhang (2013). The first intelligent human welder modeling and control method was accomplished using an artificial neural network (ANN). Again, the same TIG welding process and laser vision system was used for experimentation, but the data structure was modeled different. The input parameters consist of the real time 3D pool surface quality extracted (weld pool width, length, and convexity). An Adaptive Neuro-Fuzzy Inference System (ANFIS) technique was used to learn the welding process and output the current, with an RMS error of 0.517A. Once the model of the system was learned, the input and output parameters were swapped in order to control and optimize weld quality. Given a desired weld bead width, the algorithm suggests an adjustment to the welding parameters (current, speed, arc length). This study established a foundation to add human welder's intelligence into a robotic welding system.

The ANFIS model based predictive control uses nonlinear optimization, which are not preferred for online industrial applications. Liu and Y. Zhang (2014) then used the nonlinear ANFIS model to train the system and a linear, model predictive control (MPC) algorithm to optimize the process. Open-loop control experiments were conducted to show the controller's ability to achieve a desired weld bead quality under various disturbances and initial conditions.

Eventually, Liu, Y. Zhang, and Y. Zhang (2015) accomplished a modeling and control technique for an online intelligent arc welding system. A dynamic nonlinear



ANFIS model was used to train the system and utilized as a nonlinear controller. This technique achieved faster response time than the linear system used by Liu and Y. Zhang (2014). The achievement from a supervised learning system to a reinforcement learning system makes this algorithm useful for practical industry applications.

Wang and Li (2014) were able to borrow data from the University of Kentucky's lab and apply three different BP-ANNs to optimize weld bead quality. Wang's model was based off of 11 input data parameters: weld pool length, width, half length, half width, height, section area, concavity, radius, current, arc length, and speed. The output for each system was backside weld bead width and height. The model was trained using a back-propagation neural network (BPNN), a principle component analysis based back-propagation neural network (PCABPNN), and a global best adaptive mutation particle swarm optimization based back-propagation neural network (GBAMPSO-BPNN) model. The GBAMPSO-BPNN model was capable of predicting the weld bead width, with an RMS error of 0.3872mms.

Baskoro, Tandian, Haikal, Edyanto, & Saragih (2016) also applied a BP-ANN to analyze an automated TIG welding process on stainless steel. A stepper motor was used to traverse the workpiece at a constant speed and automate the process. A charge-coupled device (CCD) camera was used to measure the top weld bead width and a ruler was used to measure the backside weld bead width. Experiments were conducted at a constant speed and constant current while the CCD measured the top bead width. The ANN was used to train the model and predict the backside weld bead quality. Baskoro et al. provide minimal description of the ANN technique other than the fact that it uses back-propagation. For a target backside weld bead width of 3mm, an absolute error of 0.11mm,

0.09mm, and 0.12mm is achieved for only three experiments. This experimental design using constant current and speed does not show much promise in modeling a dynamic welding process with changing speed or current.

Another ANN approach by Vinas, Cabrera, and Juarez (2016) was modeled after an automated MIG welding process using a Fuzzy ARTMAP technique. The architecture of the ANN uses a combination of Fuzzy Logic and Adaptive Resonance Theory. Experiments were conducted using a KUKA industrial robot to vary the input parameters (arc distance, speed, and current). A CCD camera was used to measure the output weld bead height and width. Automated welding, ANN training, and ANN testing were all conducted online in 4.5minutes. An average prediction error of 0.169mms was achieved.

A deep neural network (DNN) approach was used by Keshmiri, Zheng, Feng, Pang, and Chew (2015) to estimate weld bead quality of a MIG welding, SMAW welding, and TIG welding system. DNN is simply the parallel use of many ANNs. In Keshmiri et al.'s design four-hidden-layer architecture; the first three layers utilize the sigmoid function and the fourth layer uses a linear transformation to produce the final output of the system. Input parameters (voltage, current, speed, and wire-speed were used to predict the output parameters (depth of penetration and weld bead width). RMSE of the predicted width for four different datasets were achieved: 0.115mm, 0.15mm, 0.153mm, and 0.124mm. The study shows that DNN's are capable of modeling various welding process and produce good results with a limited number of data points.

### Support Vector Machines

While NNs have proven to dominate the welding optimization research, others have used statistical learning strategies to model the process. Li, Gao, Wu, Hu, and Wang first used a Support Vector machine to classify the weld quality of a Metal Active Gas (MAG) welding process. In this process, the weld shape was not a straight-line weld like all other researchers, but the input and output variables were similar. Li et al. kept arc distance, speed, gas flow, and at constant settings while changing the one input variable current. The goal was to model the relationship with the output weld quality, measured by a vision-based sensor. The classifier was capable of successfully predicting the groove state, or weld bead quality, 85% of the time.

So, then Dong, Huff, Cong, Zhang, and Chen (2016) adopted the classification technique and designed their own Support Vector machine algorithm. TIG welding experiments were conducted with Liu et al.'s (2013) model for predicting characteristic performance was used: the input variables were welding parameters, previous welding parameters, and previous characteristic performance, while the output variable was the current characteristic performance. More specifically; Dong and Huff's input variables were current, previous current and previous weld bead width while the output variable was weld bead width. Classification of weld bead width was successfully predicted at 95%. Classifiers have proven to model the welding process for a range of values, but not a discrete value.

### Gaussian Process Regression

Next, Dong, Cong\*, Liu, Zhang, and Chen (2016) used a regression technique to model the welding process using Gaussian Process Regression (GPR). GPR regression of

welding data had briefly been investigated by D. Sterling, T. Sterling, Zhang, and Chen (2015) at Texas State University. The GPR was first used to model the welding process and optimize the parameters for weld bead strength. Dong was able to design a more complex algorithm using Liu and Zhang's (2014) modeling technique for predicting characteristic performance. Using input variables: previous width, previous current, and previous speed; Dong modeled the relationship with output variables width and convexity. A maximum prediction error and minimum prediction error of 0.1017mm and 0.0067mm were achieved for width. And a maximum prediction error and minimum prediction error of 0.0182mm and 0.0024mm were achieved for convexity. The GPR proved capability of modeling the welding process for a discrete mean value with a specified variance. Further research by Dong et al. (2017) was done to equip the GPR algorithm with a Bayesian Optimization Algorithm (BOA). Upper confidence bound and lower confidence bound techniques were applied to the predicted mean and variance. By incorporating the BOA, Dong was then capable of modeling the process in real time.

### Origination of Thesis

Artificial Intelligence has increased industrial robot welding capabilities through several machine learning algorithms. Neural Networks based off back propagation have dominated the welding process modeling and optimization. However, there is a lack of other machine learning techniques used to solve the problem. Dong and Huff used other techniques such as SVM and GPR to model and predict the weld bead quality successfully.

Table 1. Machine Learning Algorithms used to Model the Welding Process						
Author(s)	Algorithm	Technique	Welding Process	Material	Output	Error
W. Zhang, Y. Zhang (2012)	Regression	Least Square	TIG	steel	width	$s^2 = 0.39\text{mm}^2$
Liu, W. Zhang, Y. Zhang (2013)	ANN	Fuzzy Logic	TIG	steel	current	RMSE = 0.67A max = 3.83A
Liu, Y. Zhang (2014)	ANN	Fuzzy Logic	TIG	steel	width	max = 0.5mm
Liu, W. Zhang, Y. Zhang (2015)	ANN	Fuzzy Logic	TIG	steel	width	RMSE = 0.60A max = 4.17A
Wang, Li (2014)	ANN	Back Propagation	arc, smaw, TIG	steel	width	RMSE = 0.3872
Keshmiri et al. (2015)	DNN	Back Propagation	TIG, SMAW	steel, SS304	width	.124mm or 2.52%
Baskaro et al. (2016)	ANN	Back Propagation	TIG	SS304	width	.09mm or 2%
Vinas et al. (2016)	ANN	Back Propagation	MIG	steel	width	0.169mm avg

Table 1. Continued						
Author(s)	Algorithm	Technique	Welding Process	Material	Output	Error
Li et al. (2014)	Classification	SVM	MIG	steel	width	15%
Sterling et al. (2015)	Regression	GPR	TIG	steel	optimum parameters	13 experiments
Dong, et al. (2016)	Classification	SVM	TIG	steel	width	5% error
Dong et al. (2016)	Regression	GPR	TIG	steel	width	maE = 0.1017mm min = 0.0067mm
Dong et al. (2017)	Regression	GPR	TIG	steel	width	max = 3.9% miE = 0.27%

We propose a machine learning algorithm, GPR, to model the robotic welding process and predict change in welding parameters. We tackle this intelligent welding problem in the following order: First, we modify the classical welding model approach and create our modified dataset of inputs and output variables. Second, a GPR method is presented to model the dataset and predict future change in welding current. Third, aluminum TIG welding experiments are conducted using an industrial robot to control welding parameters. Fourth, the experimental data is used to train the algorithm offline and model the process. Finally, verification experiments are conducted to verify the algorithms accuracy.

### III. PROPOSED SOLUTION

#### Process Modeling

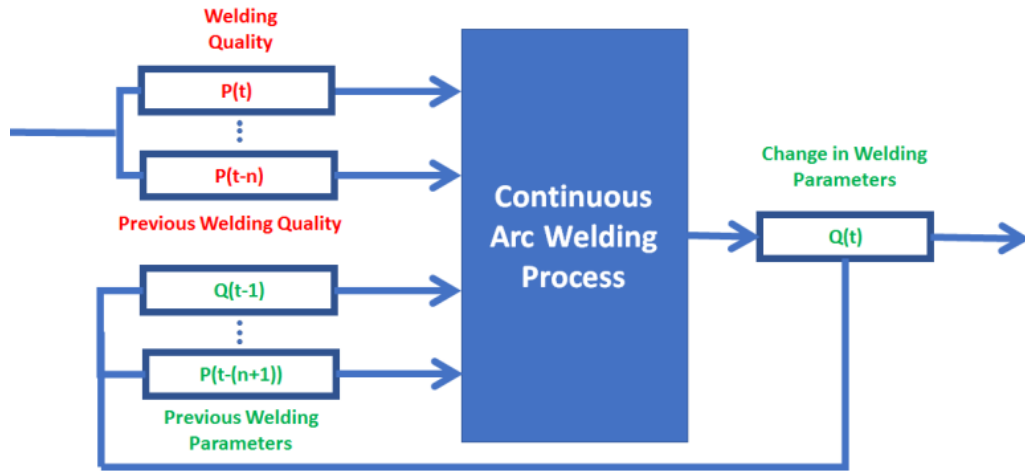
Arc welding is a dynamic process with many complex variables that make it challenging to model. Most significantly; there are several welding parameters (WP) (current, voltage, speed, arc distance, etc.) that determine the quality of the weld bead (WQ) (width, depth of penetration, convexity, tensile strength, etc.) The input and output parameters strongly correlate with each other; however, it is a nonlinear relationship. Also, the process involves uncertainties including metallurgy, heat transfer, chemical reaction, arc physics, and electromagnetism. Hence why Wang and Li (2014) label the arc welding process as a multi-input, multi-output (MIMO), nonlinear, time-varying, and strong coupled process.

In order to model the process, we must first understand the skill needed by human welders. The principle of human welder's intelligence and control is briefly described: Given a welding task of joining two metals together at a joint, the human must first evaluate the properties of the workpiece material, the workpiece thickness, and determine a desired weld bead quality ( $WQ_d$ ). Based off prior experience, some initial estimation of welding parameters (WP) is determined. After an initial welding arc is struck on the workpiece, the welder evaluates the actual weld bead quality (WQ) with his eyes. Over time,  $t$ , the real time observed data  $WQ(t)$ , prior observed data  $WQ(t-1)$ , and prior welding parameters  $WP(t-1)$  used to determine the necessary control action, or change in WP. The change in WP is human skill required for controlling good quality welds and a vital skill industrial robots lack.

Considering the complexity of the process and how skilled manual welders control WP, the welding skill modeling problem can be solved by modifying the dataset. For a continuous welding process with a desired weld bead quality ( $WQ_d$ ), the required change in welding parameters WP can highly rely on their previous value and previous weld quality:

$$WP(t) = f(WP(t-1), WQ(t), WQ(t-1)) + w \quad (1)$$

Where  $w$  is noise or uncertainties. The concept can be described in Fig 7.



**Fig 7. Arc Welding Process Model for Predicting Welding Parameters**

Using Liu et al.'s (2013) modeling method for human intelligence, or welding skill, the data further can be organized into a multivariate-dataset  $[X, y]$  for any finite set of data points,  $n$ . The input matrix is:

$$\begin{aligned} X = & [(WP(t-1), WQ(t), WQ(t-1)), \\ & (WP(t-2), WQ(t-1), WQ(t-2)), \dots, \\ & (WP(t-n), WQ(t-(n+1)), WQ(t-n))] \end{aligned} \quad (2)$$



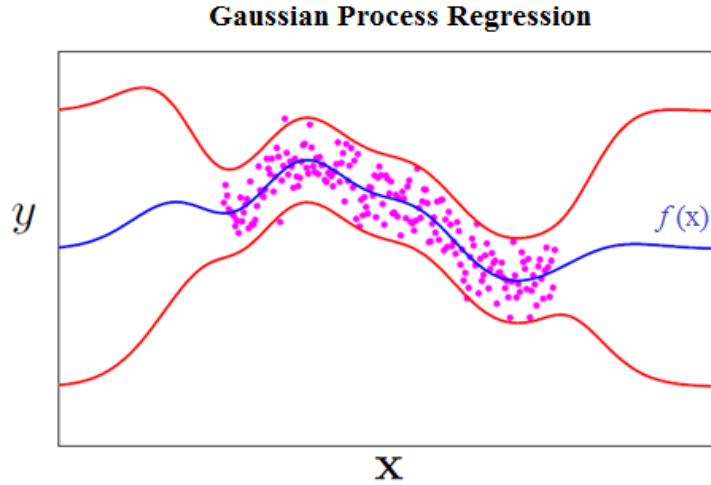
The output matrix includes only one  $n \times 1$  vector:

$$\mathbf{y} = [\text{WP}(t), \text{WP}(t-1), \dots, \text{WP}(t-n)] \quad (3)$$

Once a dataset  $[\mathbf{X}, \mathbf{y}]$  of a process is obtained a model can be trained to learn the relationship between the inputs and output.

### Gaussian Process Regression

Gaussian Process Regression (GPR) is a statistical method used to obtain a probabilistic model of a complex process. For a finite number of data points, there exists a multivariate Gaussian distribution function  $f(\mathbf{x})$  for each input, defined by its mean and variance. The Gaussian process can be defined as a collection of many joint probabilistic distribution functions over time to represent the process, as seen in Fig 8.



**Fig 8. Gaussian Process Regression (Snelson, 2006)**

This non-parametric modeling technique uses second order statistics to model a complex process with noisy observations and uncertainties. The “kernel” trick uses different covariance functions to model various forms of data trends, such as linear, sinusoidal, parabolic, constant, etc. Also, this technique is not bounded by a number of

input parameters. Hence GPR is a robust tool that can be used to model the multi-input, multi-output (MIMO), nonlinear, time-varying, and strong coupled TIG welding process.

For a Gaussian Process  $f(\mathbf{x})$ , a set of multivariate Gaussian random variables  $F = \{f(\mathbf{x}_1), f(\mathbf{x}_2), \dots, f(\mathbf{x}_N)\}$  can be defined over  $X$  with any finite set of  $N$  points  $\{\mathbf{x}_i \in X\}_{i=1}^N$  where  $f(\mathbf{x}_i)$  has the value of the latent function  $f(\mathbf{x})$  at  $\mathbf{x}_i \in X$  and  $X$  is defined over  $\mathbb{R}^D$ .  $f(\mathbf{x})$  is completely specified by its mean function  $m(\mathbf{x})$  and covariance function  $k(\mathbf{x}, \mathbf{x}')$ :  $f(\mathbf{x}) \sim \mathcal{GP}(m(\mathbf{x}), k(\mathbf{x}, \mathbf{x}'))$  where  $\mathbf{x}$  and  $\mathbf{x}'$  are two arbitrary variables in  $X$ .

For a model  $y = f(\mathbf{x}) + w$  and  $w \sim N(0, \sigma_n^2)$ , the covariance function is  $\text{cov}(y_i, y_j) = k(\mathbf{x}_i, \mathbf{x}_j) + \sigma_n^2 \delta_{ij}$ , where  $\delta_{ij}$  is the Kronecker delta which is one, if  $i = j$  and zero otherwise. The joint distribution of the observed data set  $(\mathbf{X}, \mathbf{y})$  and predicted data set  $(\mathbf{X}_*, \mathbf{y}_*)$  is

$$\begin{bmatrix} \mathbf{y} \\ \mathbf{y}_* \end{bmatrix} \sim N\left(0, \begin{bmatrix} K(\mathbf{X}, \mathbf{X}) + \sigma_n^2 \mathbf{I} & K(\mathbf{X}, \mathbf{X}_*) \\ K(\mathbf{X}_*, \mathbf{X}) & K(\mathbf{X}_*, \mathbf{X}_*) \end{bmatrix}\right) \quad (4)$$

Where  $K(\mathbf{X}', \mathbf{X}'')$  ( $\mathbf{X}'$  and  $\mathbf{X}''$  refer to  $\mathbf{X}$  and  $\mathbf{X}_*$ ) is the covariance matrix whose element  $K_{ij}$  in  $i_{th}$  row and  $j_{th}$  column equals to  $k(\mathbf{x}_i', \mathbf{x}_j'')$ . By deriving the conditional distribution, we can obtain:

$$(\mathbf{y}_* | \mathbf{X}, \mathbf{y}, \mathbf{X}_*) \sim N(\mu(\mathbf{y}_*), V(\mathbf{y}_*)) \quad (5)$$

$$\mu(\mathbf{y}_*) = E[\mathbf{y}_* | \mathbf{X}, \mathbf{y}, \mathbf{X}_*] = K(\mathbf{X}_*, \mathbf{X}) [K(\mathbf{X}, \mathbf{X}) + \sigma_n^2 \mathbf{I}]^{-1} \mathbf{y} \quad (6)$$

$$V(\mathbf{y}_*) = K(\mathbf{X}_*, \mathbf{X}_*) - K(\mathbf{X}_*, \mathbf{X}) [K(\mathbf{X}, \mathbf{X}) + \sigma_n^2 \mathbf{I}]^{-1} K(\mathbf{X}, \mathbf{X}_*) \quad (7)$$

Where  $\mu(\mathbf{y}_*)$  is the predicted mean for  $\mathbf{y}_*$  and  $V(\mathbf{y}_*)$  is the predicted variance. The covariance function  $k(\mathbf{x}, \mathbf{x}')$  is a key for determining a GPR model. Among various forms of covariance functions, a commonly-used one is the Squared Exponential  $k_{SE}(\mathbf{x}, \mathbf{x}')$  which is:

$$k_{SE}(\mathbf{x}, \mathbf{x}') = \sigma^2 \exp\left(-\frac{|\mathbf{x}-\mathbf{x}'|^2}{2l^2}\right) \quad (8)$$

Where  $l$  is a characteristic length-scale factor controlling how close  $\mathbf{x}$  and  $\mathbf{x}'$  are and  $\sigma^2$  is the amplitude of the variance. For each covariance function, there are some hyperparameters  $\theta$  such as  $l$  and  $\sigma$  for  $k_{SE}$ . The goal of model construction is to find a covariance function  $k(\mathbf{x}, \mathbf{x}', \theta)$  which fits the data set  $(\mathbf{X}, \mathbf{y})$  best. Suppose  $f(\mathbf{x})$  is a candidate latent function,  $f$  in short, for the given data set, the posterior probability is:

$$p(f|\mathbf{X}, \mathbf{y}, H, \theta) = \frac{p(\mathbf{y}|\mathbf{X}, f, H, \theta) p(f|\mathbf{X}, H, \theta)}{P(\mathbf{y}|\mathbf{X}, H, \theta)} \quad (9)$$

Where  $H$  is the hypothesis on the structure of the covariance function,  $\theta$  is the hyperparameters,  $\mathbf{X}, \mathbf{y}$  are the sample data sets and

$$p(\mathbf{y}|\mathbf{X}, H, \theta) = \int p(\mathbf{y}|\mathbf{X}, f, H, \theta) p(f|\mathbf{X}, H, \theta) df \quad (10)$$

is the marginal likelihood that refers to the marginalization over the function  $f$ .

As mentioned above, in the Gaussian Process Regression  $f(\mathbf{x})$  is not given explicitly. Thus,  $p(\mathbf{y}|\mathbf{X}, H, \theta)$  actually refers to the likelihood of  $H$  and  $\theta$  given the data set  $(\mathbf{X}, \mathbf{y})$ . The Gaussian assumption makes it possible to derive the analytical solution of the log marginal likelihood:

$$\log P(\mathbf{y}|\mathbf{X}, H, \theta) = -\frac{1}{2} \log|(K + \sigma_n^2 \mathbf{I})| - \frac{1}{2} \mathbf{y}^T (K + \sigma_n^2 \mathbf{I})^{-1} \mathbf{y} - \frac{n}{2} \log 2\pi \quad (11)$$

Therefore the hyperparameters  $\theta$  in a covariance function  $H$  can be optimized by maximizing the marginal log likelihood:

$$\theta^* = \operatorname{argmax}_{\theta} \log p(\mathbf{y}|\mathbf{X}, H, \theta) \quad (12)$$

This optimization problem can be solved using different techniques such as Conjugated Gradient Algorithm or evolutionary algorithms. Nelder-Mead(Simplex)

method is utilized which is effective and uses only the value of  $\log p(\mathbf{y}|\mathbf{X},\mathbf{H},\theta)$ . Once  $k(\mathbf{x},\mathbf{x}',\theta)$  is known, equation (7) can be used to make a prediction for a new input  $\mathbf{x}^*$ .

In this paper, a kernel trick models the data form by using the sum of three separate kernels are used. The three kernels used include: the Rational Quadratic kernel, the constant kernel, and the Gaussian noise kernel. They can be defined, respectively:

$$k_{\text{SE}}(\mathbf{x},\mathbf{x}') = \sigma^2 \exp\left(-\frac{|\mathbf{x}-\mathbf{x}'|^2}{2l^2}\right) \quad (13)$$

$$k_{\text{C}}(\mathbf{x},\mathbf{x}') = \text{C} \quad (14)$$

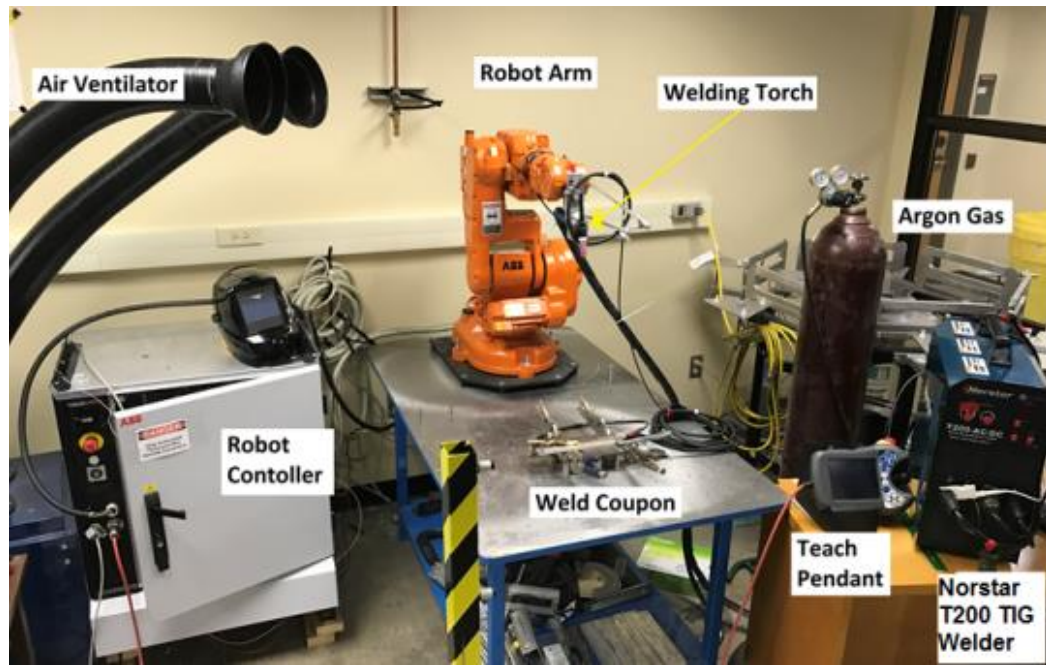
$$k_{\text{GN}}(\mathbf{x},\mathbf{x}') = \sigma_n^2 \delta_{(\mathbf{x},\mathbf{x}')} \quad (15)$$

Where the length scale  $l$ , the amplitude  $\sigma^2$ , and the Kronecker delta  $\delta$  are hyperparameters that can vary the form of the covariance function to fit the data  $[\mathbf{X},\mathbf{y}]$  best.

## IV. EXPERIMENTATION

### Robotic TIG Welding Experiments

TIG welding experiments were automated using an industrial robot to gather data for the modeling dataset and train the GPR algorithm. Further validation experiments were conducted to verify accuracy of the proposed method. The experimental system as shown in Figure 9 consists of an ABB IRB140 industrial robot with an IRC5 controller, a Coplay Norstar T200 AC/DC TIG welding machine, an air ventilation system, and 100% Argon gas.



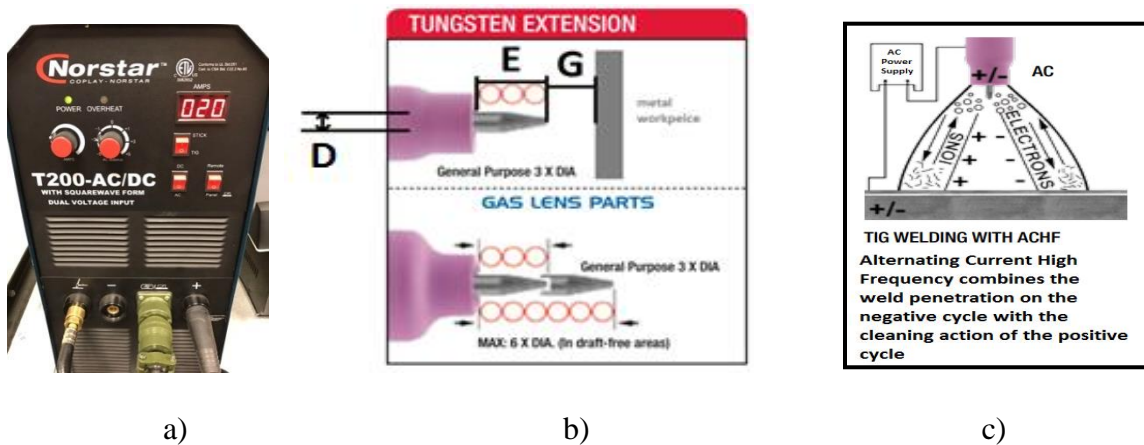
**Fig 9. Autonomous TIG Welding System**

Aluminum metal was first prepared into welding coupons. 1/8" aluminum was selected and cut into 1.5" x 10" weld coupons using a water jet machine. Then, each coupon was lightly grinded using an aluminum grinding wheel as seen in Figure 2.



**Fig 10. Aluminum Weld Coupons Before & After Grinding**

The coupons were ready for experimentation after being grinded and ridged of the aluminum oxide layer on the surface. Each coupon was clamped down and grounded before each experiment. Then, the welding machine input parameters were set to optimum settings for 1/8" aluminum, based off guidance from CK Worldwide's Technical Specifications for TIG Welding manual (2017).

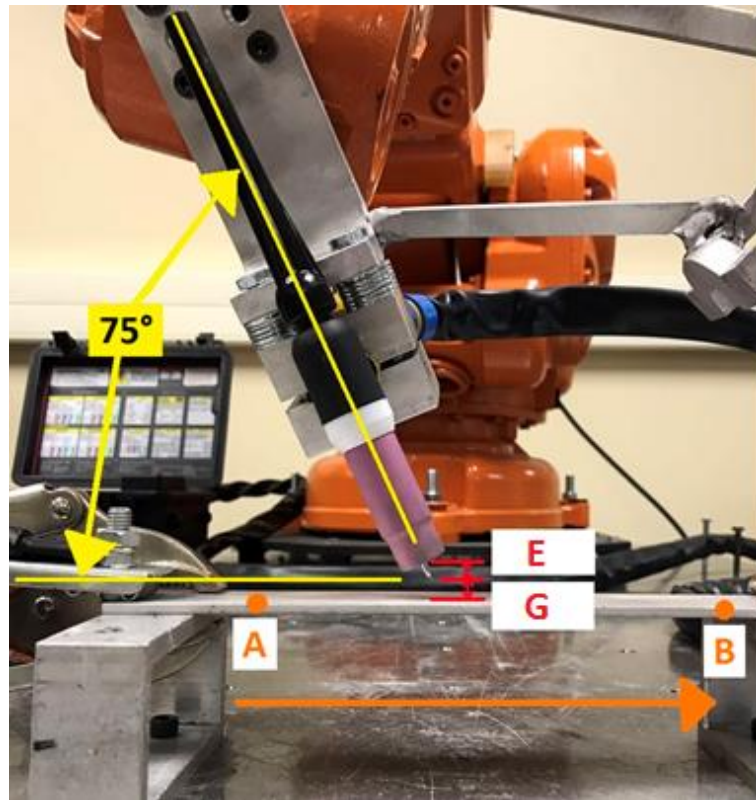


**Fig 11. Welding Machine & Input Parameters a) Norstar TIG Machine b) Torch Parameters c) AC balance. Taken from ckworldwide.com**

The Norstar welding machine was set to ACHF since the workpiece was a nonferrous metal. The AC balance was set to “-3” to provide more weld penetration and less cleaning action as seen in Fig 11c. Next, 100% pure tungsten was selected with a

diameter, measurement D in Fig. 11, of  $3/32''$ . The welding torch was setup with a #7 ceramic cup and the tungsten extension distance, or measurement E in Fig. 11, was set to  $9/32''$ . Current on the machine was set to the initial current of each experiment.

After the weld coupons were prepared and the machine parameters were set, a robot program was written using the program RobotStudio to carry out the welding experiments. ABB's robot programming language RAPID was used.



**Fig 12. Robot Program Parameters**

The welding torch was programmed to move to a point in space, point A seen in Fig.12, at the beginning of the weld coupon. The vertical torch angle was set to  $75^\circ$  from the horizontal weld plane. Then the arc distance, point G seen in Fig. 12, was set to  $0.05''$ . Finally, the welding torch was programmed to move in a straight line to point B in Fig 12 with a constant speed of  $0.1181''$ , or 3mm/s.



A total of 50 welding experiments were conducted, Fig. 14. For each experiment, the welding current was set to an initial random current value while traveling the first 3.3", then adjusted to a second random current value while traveling the next 3.3", and then adjusted to a third random current value for the last 3.3". For example, in Fig 13 the current in welding experiment #4 is initially 79A, changes to 83A, and then changes to 55A.



**Fig 13. Experiment #4**

A total of 50 welding experiments were conducted as seen in Fig 14:



**a) Experiment 1-10**

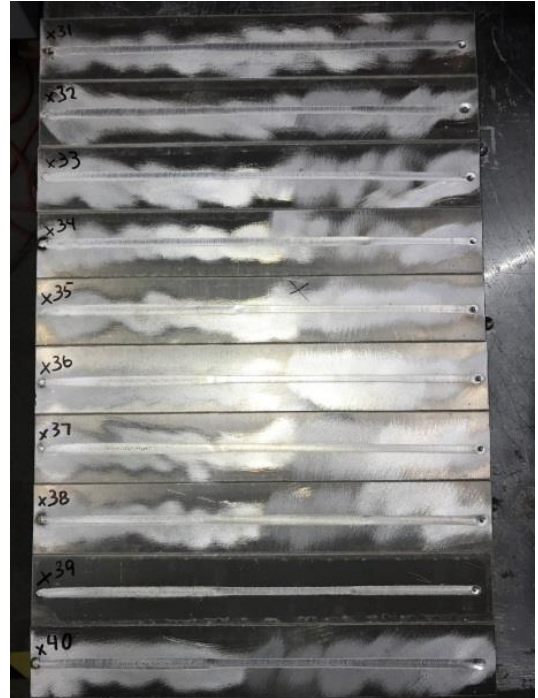


**b) Experiment 11-20**





**c) Experiment 21-30**



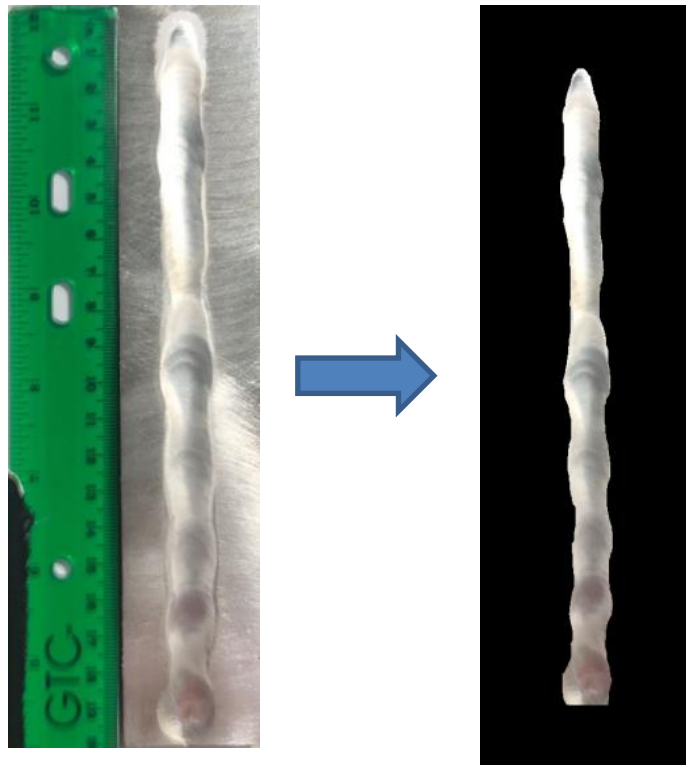
**b) Experiment 31-40**



**e) Experiment 41-50**

**Fig 14. Training Experiment Weld Coupons a) Experiments 1-10 b) Experiments 11-20 c) Experiments 21-30 d) Experiments 31-40 e) Experiments 41-50**

After the experiments were completed, an image processing code was used to measure the weld bead width.



**Fig 15. Shading in Microsoft Paint**

A 1280 x 960 pixel resolution photo was taken of the top of the weld bead. Then, Microsoft Paint was used to manually shade everything pure black in the picture that was not part of the weld bead. Using computer software Matlab, the code interposed which pixels were pure black and which were weld bead. For a given horizontal row of pixels, the number of weld bead pixels yielded the pixel width of the weld bead. The pixel width was then calibrated with the pixel length of 1" on a ruler. Finally, a weld bead width value was measured for each current value. This method was used for the first five experiments. The width was also measured using a manual set of calipers. Since the manual shading was required for image processing and the width measurements with the calipers were more straight forward, caliper measurements were performed for all the

data. For each current value, three width measurements were recorded, found in Appendix A. The width measurement's mean and variance can be found in Appendix B. Welding currents and weld bead widths from experiments 1-50, 2 datasets each, were used to create the data set  $[\mathbf{x}, \mathbf{y}]$  of size  $100 \times 4$ . The multivariable input  $[\mathbf{x}]$  has a size of  $100 \times 3$  and the output variable  $[\mathbf{y}]$  has a size  $100 \times 1$ . 90/100 randomly selected data points in the data set  $[\mathbf{x}, \mathbf{y}]$  were used to create the training data set  $[\mathbf{trainX}, \mathbf{trainY}]$  and the remaining 10/100 data points were used for the testing data set  $[\mathbf{testX}, \mathbf{testY}]$ .

Finally, five more validation experiments were performed. However, the initial current was set to some random value while traveling the first 5" and then adjusted the algorithm's predicted current value for the last 5". The previous current, current, previous width, and width were used to create the new testing data set  $[\mathbf{valX}, \mathbf{valY}]$  of size  $5 \times 4$ . The raw data can be found in Appendix C and the mean and variance can be found in Appendix D.



Fig 16. Validation Experiments #1-5

## V. RESULTS

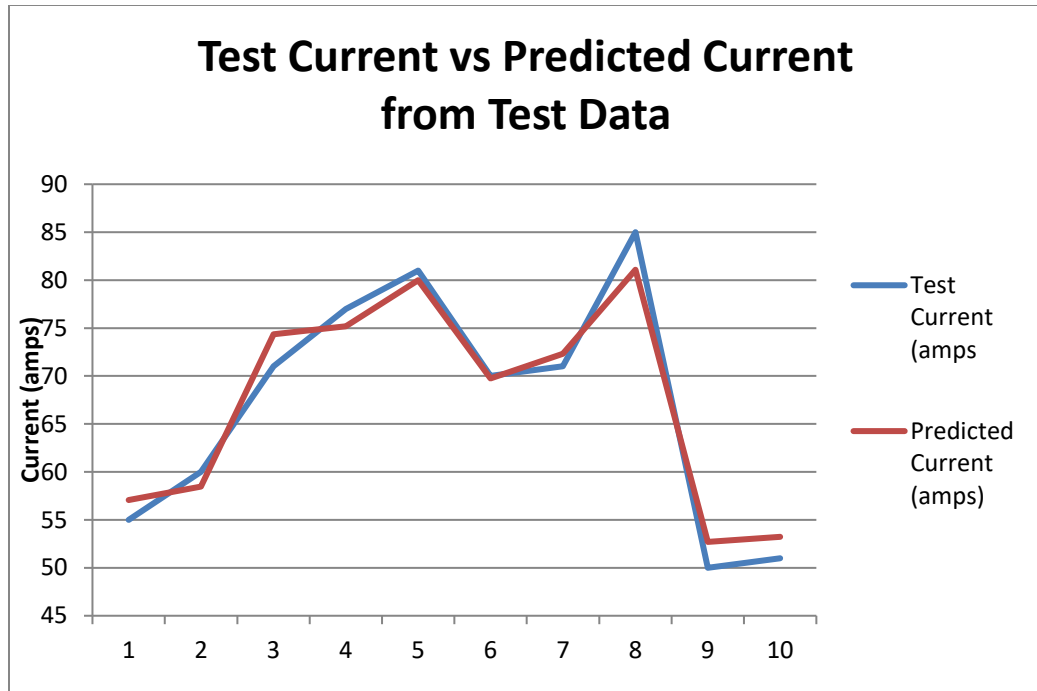
### Training Results

A modeling algorithm was written on Matlab, equipped with an open source toolbox: “Gaussian Process Regression for Machine Learning.” (Rasmussen & Nickisch, 2017) The following kernel functions were used with their respective optimal hyperparameters.

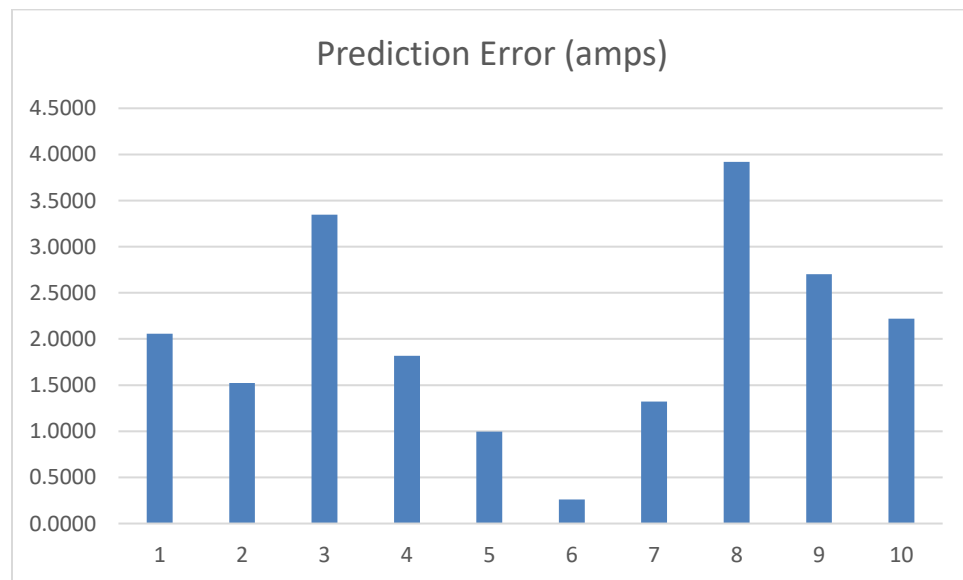
Table 2. Covariance Functions	
Name	Function
covConst	Constant
covSEiso	Squared Exponential
covNoise	Gaussian Noise

The GPR model was trained using [**trainX**,**trainY**]. Applying the GPR model to the input [**testX**], predictions were made of output variable [**testY**]. The prediction results are shown in Table 3.

<b>Table 3. Predicted Current and Error of Test Data Set</b>						
<b>Exp.</b>	<b>Previous Width (inches)</b>	<b>Previous Current (amps)</b>	<b>Width (inches)</b>	<b>Current (amps)</b>	<b>Predicted Current (amps)</b>	<b>Error (amps)</b>
91	0.1550	62	0.1350	55	57.0576	2.0576
92	0.1950	78	0.1420	60	58.4784	1.5216
93	0.2100	83	0.1900	71	74.3469	3.3469
94	0.1700	65	0.1980	77	75.1829	1.8171
95	0.1650	68	0.2100	81	80.0032	0.9968
96	0.1460	57	0.1750	70	69.7404	0.2596
97	0.1910	76	0.1880	71	72.3215	1.3215
98	0.1870	75	0.2160	85	81.0823	3.9177
99	0.2000	80	0.1220	50	52.7012	2.7012
100	0.0165	65	.0125	51	53.2198	2.2198



**Figure 17. Test Current vs Predicted Current from Test Data**



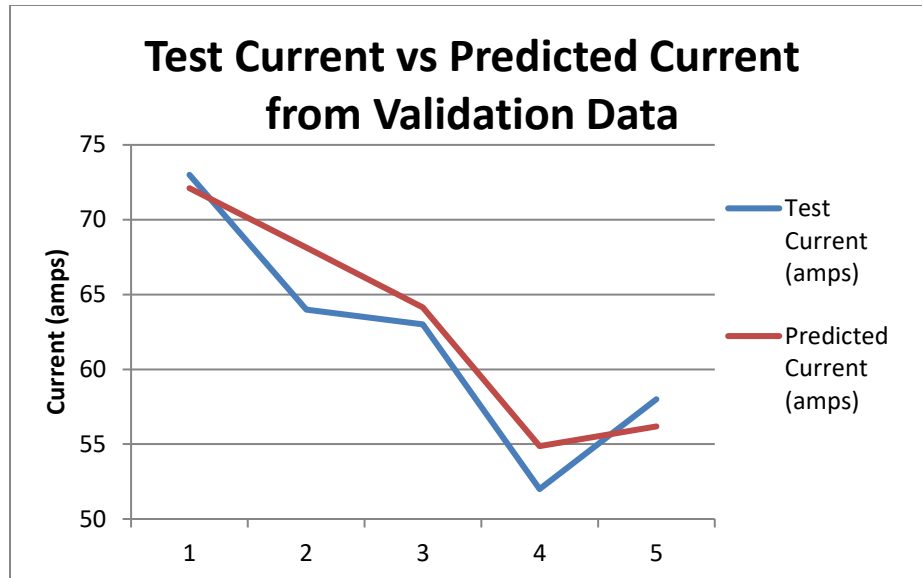
**Figure 18. Prediction Error from Test Data**

Ten predictions of the width were made using the trained GPR model. The root mean square error for the test data is 2.2679A and the maximum error is 3.9177A. These results show the algorithm is capable of predicting current accurately.

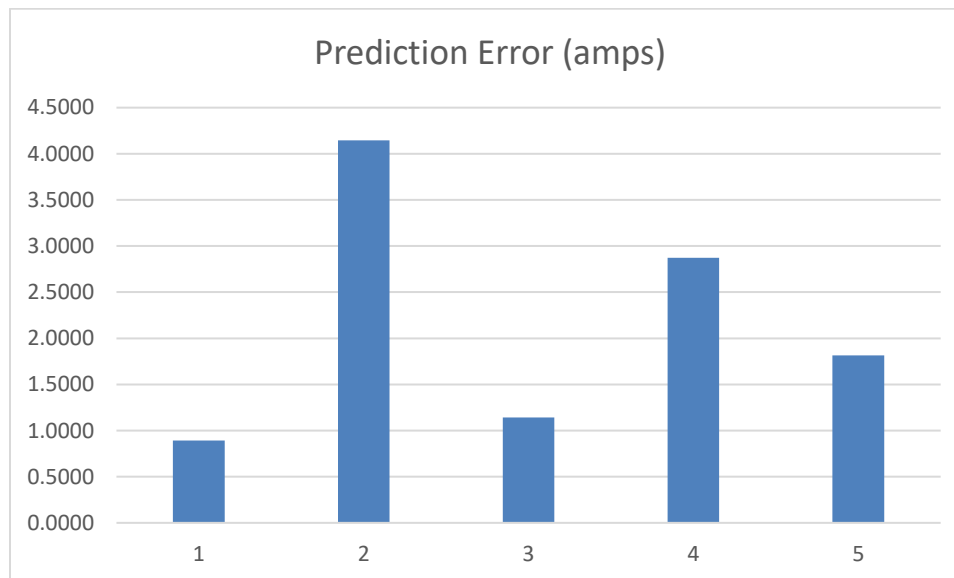
### Validation Results

In order to verify the GPR model is accurate and the predictions on the training data weren't a mistake, validation experiments were run. The GPR model, trained from the training dataset, was used to make predictions on the validation dataset. Given the input [**valX**], predictions were made of output variable [**testY**]. The results are shown in Table 4.

<b>Table 4. Predicted Current and Error of Validation Data Set</b>						
<b>Exp.</b>	<b>Previous Width (inches)</b>	<b>Previous Current (amps)</b>	<b>Width (inches)</b>	<b>Test Current (amps)</b>	<b>Predicted Current (amps)</b>	<b>Error (amps)</b>
v1	0.1400	56	0.1850	73	72.1065	0.8935
v2	0.2410	81	0.1620	64	68.1439	4.1439
v3	0.2300	78	0.1640	63	64.1410	1.1410
v4	0.2430	83	0.1450	58	56.1850	1.8150
v5	0.1800	68	0.1200	52	54.8713	2.8713



**Figure 19. Test Current vs Predicted Current from Validation Data**



**Figure 20. Prediction Error from Validation Data**

The average mean square error for the validation data is 2.4824A and the maximum error is 4.1439A. Results indicate the proposed method can accurately predict the welding current based off previous welding current, previous weld bead width, and current weld bead width.



## VI. CONCLUSION

### Contribution

In this research, an intelligent automated TIG welding system is developed, incorporating a welding manufacturing process, industrial robot automation, and a machine learning algorithm. A GPR algorithm is proposed to model the welding process and extract welder's skill. To demonstrate the effectiveness, we perform aluminum TIG welding experiments with an industrial robot. The robot is capable of controlling welding parameters and producing a consistent dataset. The dataset is further modified to yield future changes in welding current for a desired weld bead thickness. The GPR technique uses the modified dataset to train the algorithm and make prediction. Validation experiments were performed for verification.

Given a desired weld bead thickness, the required change in current can be estimated with good accuracy using the GPR method. The RMSE and maximum prediction error are 2.4824A and 4.1439A, respectively. This automated welder response model can deal well with noise and uncertainties in the TIG welding process. The model can control the TIG welding process by adjusting the current parameter to maintain a consistent weld bead width. To our knowledge, this is the first machine learning algorithm used to model aluminum TIG welding.

### Future Work

Future investigations in this area may: 1) include variations in speed, arc distance, and material thickness; 2) develop an online system capable of sensing and making predictions efficiently enough for real time application; 3) attach a wire feeder to the autonomous welding system and weld two pieces of metal together for industrial

solutions; 4) apply the GPR algorithm to other dynamic manufacturing processes and also other fields of study, such as economics or statistics data sets.

## APPENDIX SECTION

### Appendix A. Mean and Variance of Width for Training Experiments

Exp. No.	Current 1 (amps)	Width 1 (inches)	Width 2 (inches)	Width 3 (inches)	Current 2 (amps)	Width 3 (inches)	Width 4 (inches)	Width 5 (inches)
1	70	0.1490	0.1530	0.1500	50	0.0970	0.1000	0.0990
2	79	0.1820	0.1880	0.1860	63	0.1480	0.1420	0.1520
3	57	0.1240	0.1300	0.1260	77	0.1910	0.1930	0.1960
4	79	0.2000	0.1960	0.2020	83	0.2380	0.2400	0.2350
5	66	0.1450	0.1440	0.1450	75	0.1690	0.1760	0.1690
6	82	0.2090	0.2120	0.2060	67	0.1530	0.1500	0.1570
7	62	0.1510	0.1480	0.1520	53	0.1260	0.1220	0.1290
8	68	0.1620	0.1590	0.1600	51	0.1140	0.1120	0.1130
9	77	0.2020	0.1960	0.1920	83	0.2140	0.2150	0.2200
10	50	0.1200	0.1110	0.1150	70	0.1690	0.1580	0.1600
11	85	0.2180	0.2220	0.2150	50	0.1100	0.1070	0.1060
12	78	0.1950	0.1920	0.1940	51	0.1140	0.1120	0.1170
13	54	0.1200	0.1150	0.1120	75	0.1800	0.1780	0.1840
14	59	0.1440	0.1380	0.1440	71	0.1780	0.1750	0.1710
15	68	0.1670	0.1700	0.1610	76	0.1950	0.2000	0.1990
16	56	0.1340	0.1380	0.1300	75	0.2010	0.1900	0.1940
17	69	0.1666	0.1660	0.1620	50	0.1220	0.1270	0.1250
18	73	0.1800	0.1690	0.1760	68	0.1650	0.1670	0.1740
19	65	0.1620	0.1590	0.1500	76	0.2050	0.1900	0.2020

20	55	0.1210	0.1190	0.1340	68	0.1690	0.1680	0.1720
21	68	0.1700	0.1650	0.1650	79	0.2070	0.2050	0.2100
22	80	0.2150	0.2170	0.2140	59	0.1350	0.1350	0.1400
23	68	0.1790	0.1780	0.1780	81	0.2130	0.2100	0.2150
24	68	0.1660	0.1650	0.1620	53	0.1170	0.1140	0.1150
25	65	0.1660	0.1670	0.1650	52	0.1250	0.1160	0.1200
26	67	0.1710	0.1680	0.1660	56	0.1250	0.1320	0.1270
27	51	0.2250	0.2220	0.2300	61	0.1450	0.1410	0.1460
28	57	0.1300	0.1350	0.1330	83	0.2270	0.2190	0.2250
29	75	0.2050	0.2040	0.1960	84	0.2410	0.2420	0.2450
30	77	0.2100	0.2280	0.2160	56	0.1440	0.1320	0.1300
31	64	0.1380	0.1460	0.1400	85	0.1940	0.1980	0.1940
32	72	0.1650	0.1800	0.1700	55	0.1300	0.1280	0.1290
33	63	0.1420	0.1500	0.1500	51	0.1220	0.1140	0.1240
34	63	0.1440	0.1490	0.1520	81	0.2040	0.2090	0.2070
35	80	0.2020	0.2100	0.2090	62	0.1500	0.1520	0.1540
36	76	0.1920	0.2040	0.2020	52	0.1290	0.1310	0.1270
37	82	0.2250	0.2270	0.2180	67	0.1750	0.1760	0.1710
38	62	0.1480	0.1510	0.1480	78	0.1920	0.1990	0.2050
39	75	0.1900	0.2050	0.2030	51	0.1370	0.1390	0.1360
40	85	0.2130	0.2150	0.2220	66	0.1460	0.1520	0.1500
41	57	0.1330	0.1260	0.1240	62	0.1460	0.1500	0.1540
42	84	0.2270	0.2190	0.2270	78	0.1960	0.2040	0.2020

43	56	0.1450	0.1500	0.1370	83	0.2070	0.2120	0.2150
44	83	0.2150	0.2300	0.2280	65	0.1650	0.1690	0.1600
45	56	0.1390	0.1280	0.1220	68	0.1620	0.1720	0.1750
46	77	0.2020	0.2170	0.1950	57	0.1470	0.1480	0.1380
47	60	0.1560	0.1510	0.1520	76	0.1920	0.1960	0.1990
48	68	0.1770	0.1800	0.1820	75	0.1920	0.1950	0.1940
49	53	0.1220	0.1270	0.1250	80	0.2200	0.2140	0.2120
50	57	0.1290	0.1370	0.1410	65	0.1590	0.1690	0.1610
51	50	0.0970	0.1000	0.0990	90	0.2980	0.2150	0.2140
52	63	0.1480	0.1420	0.1520	85	0.2280	0.2220	0.2300
53	77	0.1910	0.1930	0.1960	60	0.1550	0.1610	0.1630
54	83	0.2380	0.2400	0.2350	55	0.1420	0.1400	0.1410
55	75	0.1690	0.1760	0.1690	60	0.1350	0.1340	0.1410
56	67	0.1530	0.1500	0.1570	55	0.1160	0.1170	0.1170
57	53	0.1260	0.1220	0.1290	78	0.1820	0.1850	0.1800
58	51	0.1140	0.1120	0.1130	81	0.1900	0.1960	0.1890
59	83	0.2140	0.2150	0.2200	74	0.1850	0.2000	0.1920
60	70	0.1690	0.1580	0.1600	77	0.1930	0.1960	0.1990
61	50	0.1100	0.1070	0.1060	71	0.1590	0.1630	0.1750
62	51	0.1140	0.1120	0.1170	82	0.1950	0.2000	0.2050
63	75	0.1800	0.1780	0.1840	57	0.1470	0.1500	0.1520
64	71	0.1780	0.1750	0.1710	52	0.1310	0.1350	0.1250
65	76	0.1950	0.2000	0.1990	53	0.1340	0.1380	0.1400

66	75	0.2010	0.1900	0.1940	81	0.2100	0.2110	0.2040
67	50	0.1220	0.1270	0.1250	72	0.1820	0.1850	0.1910
68	68	0.1650	0.1670	0.1740	61	0.1530	0.1500	0.1620
69	76	0.2050	0.1900	0.2020	56	0.1440	0.1410	0.1500
70	68	0.1690	0.1680	0.1720	75	0.1920	0.1880	0.2000
71	79	0.2070	0.2050	0.2100	83	0.1250	0.1150	0.1260
72	59	0.1350	0.1350	0.1400	69	0.1670	0.1680	0.1700
73	81	0.2130	0.2100	0.2150	52	0.1250	0.1250	0.1300
74	53	0.1170	0.1140	0.1150	83	0.2100	0.2050	0.2150
75	52	0.1250	0.1160	0.1200	76	0.1850	0.1880	0.1950
76	56	0.1250	0.1320	0.1270	84	0.2050	0.2000	0.2100
77	61	0.1450	0.1410	0.1460	79	0.1920	0.1940	0.2000
78	83	0.2270	0.2190	0.2250	55	0.1460	0.1420	0.1440
79	84	0.2410	0.2420	0.2450	72	0.1950	0.2100	0.2020
80	56	0.1440	0.1320	0.1300	66	0.1640	0.1620	0.1570
81	85	0.1940	0.1980	0.1940	71	0.1740	0.1790	0.1770
82	55	0.1300	0.1280	0.1290	81	0.1920	0.1890	0.1780
83	51	0.1220	0.1140	0.1240	69	0.1570	0.1590	0.1480
84	81	0.2040	0.2090	0.2070	55	0.1370	0.1370	0.1410
85	62	0.1500	0.1520	0.1540	71	0.1700	0.1760	0.1820
86	52	0.1290	0.1310	0.1270	67	0.1570	0.1620	0.1600
87	67	0.1750	0.1760	0.1710	59	0.1510	0.1470	0.1540
88	78	0.1920	0.1990	0.2050	63	0.1940	0.1920	0.1890

89	51	0.1370	0.1390	0.1360	69	0.1820	0.1790	0.1800
90	66	0.1460	0.1520	0.1500	80	0.1840	0.1890	0.1950
91	62	0.1460	0.1500	0.1540	55	0.1390	0.1320	0.1270
92	78	0.1960	0.2040	0.2020	60	0.1500	0.1460	0.1490
93	83	0.2070	0.2120	0.2150	71	0.1970	0.1880	0.1980
94	65	0.1650	0.1690	0.1600	77	0.2050	0.2020	0.1980
95	68	0.1620	0.1720	0.1750	81	0.2000	0.2060	0.2040
96	57	0.1470	0.1480	0.1380	70	0.1760	0.1720	0.1800
97	76	0.1920	0.1960	0.1990	71	0.1880	0.1900	0.1850
98	75	0.1920	0.1950	0.1940	85	0.2150	0.2120	0.2190
99	80	0.2200	0.2140	0.2120	50	0.1320	0.1220	0.1230
100	65	0.1590	0.1690	0.1610	51	0.1240	0.1210	0.1260

---

### Appendix B. Mean and Variance of Width for Training Experiments

Exp.	Current	Mean	$\sigma^2$	Current	Mean	$\sigma^2$
No.	1	Width 1,2,3	(inches *	2	Width 4,5,6	(inches*
	(amps)	(inches)	(10 <sup>6</sup> ))	(amps)	(inches)	(10 <sup>6</sup> ))
1	70	0.1507	4.333	50	0.0987	2.333
2	79	0.1853	9.333	63	0.1473	25.333
3	57	0.1267	9.333	77	0.1933	6.333
4	79	0.1993	9.333	83	0.2377	6.333
5	66	0.1447	0.333	75	0.1713	16.333
6	82	0.2090	9.000	67	0.1533	12.333
7	62	0.1503	4.333	53	0.1257	12.333
8	68	0.1603	2.333	51	0.1130	1.000
9	77	0.1967	25.333	83	0.2163	10.333
10	50	0.1153	20.333	70	0.1623	34.333
11	85	0.2183	12.333	50	0.1077	4.333
12	78	0.1937	2.333	51	0.1143	6.333
13	54	0.1157	16.333	75	0.1807	9.333
14	59	0.1420	12.000	71	0.1747	12.333
15	68	0.1660	21.000	76	0.1980	7.000
16	56	0.1340	16.000	75	0.1950	31.000
17	69	0.1649	6.253	50	0.1247	6.333
18	73	0.1750	31.000	68	0.1687	22.333
19	65	0.1570	39.000	76	0.1990	63.000



---

20	55	0.1247	66.333	68	0.1697	4.333
21	68	0.1667	8.333	79	0.2073	6.333
22	80	0.2153	2.333	59	0.1367	8.333
23	68	0.1783	0.333	81	0.2127	6.333
24	68	0.1643	4.333	53	0.1153	2.333
25	65	0.1660	1.000	52	0.1203	20.333
26	67	0.1683	6.333	56	0.1280	13.000
27	51	0.2257	16.333	61	0.1440	7.000
28	57	0.1327	6.333	83	0.2237	17.333
29	75	0.2017	24.333	84	0.2427	4.333
30	77	0.2180	84.000	56	0.1353	57.333
31	64	0.1413	17.333	85	0.1953	5.333
32	72	0.1717	58.333	55	0.1290	1.000
33	63	0.1473	21.333	51	0.1200	28.000
34	63	0.1483	16.333	81	0.2067	6.333
35	80	0.2070	19.000	62	0.1520	4.000
36	76	0.1993	41.333	52	0.1290	4.000
37	82	0.2233	22.333	67	0.1740	7.000
38	62	0.1490	3.000	78	0.1987	42.333
39	75	0.1993	66.333	51	0.1373	2.333
40	85	0.2167	22.333	66	0.1493	9.333
41	57	0.1277	22.333	62	0.1500	16.000
42	84	0.2243	21.333	78	0.2007	17.333

---

---

43	56	0.1440	43.000	83	0.2113	16.333
44	83	0.2243	66.333	65	0.1647	20.333
45	56	0.1297	74.333	68	0.1697	46.333
46	77	0.2047	126.333	57	0.1443	30.333
47	60	0.1530	7.000	76	0.1957	12.333
48	68	0.1797	6.333	75	0.1937	2.333
49	53	0.1247	6.333	80	0.2153	17.333
50	57	0.1357	37.333	65	0.1630	28.000
51	50	0.0987	2.333	90	0.2423	2324.333
52	63	0.1473	25.333	85	0.2267	17.333
53	77	0.1933	6.333	60	0.1597	17.333
54	83	0.2377	6.333	55	0.1410	1.000
55	75	0.1713	16.333	60	0.1367	14.333
56	67	0.1533	12.333	55	0.1167	0.333
57	53	0.1257	12.333	78	0.1823	6.333
58	51	0.1130	1.000	81	0.1917	14.333
59	83	0.2163	10.333	74	0.1923	56.333
60	70	0.1623	34.333	77	0.1960	9.000
61	50	0.1077	4.333	71	0.1657	69.333
62	51	0.1143	6.333	82	0.2000	25.000
63	75	0.1807	9.333	57	0.1497	6.333
64	71	0.1747	12.333	52	0.1303	25.333
65	76	0.1980	7.000	53	0.1373	9.333

---

---

66	75	0.1950	31.000	81	0.2083	14.333
67	50	0.1247	6.333	72	0.1860	21.000
68	68	0.1687	22.333	61	0.1550	39.000
69	76	0.1990	63.000	56	0.1450	21.000
70	68	0.1697	4.333	75	0.1933	37.333
71	79	0.2073	6.333	83	0.1220	37.000
72	59	0.1367	8.333	69	0.1683	2.333
73	81	0.2127	6.333	52	0.1267	8.333
74	53	0.1153	2.333	83	0.2100	25.000
75	52	0.1203	20.333	76	0.1893	26.333
76	56	0.1280	13.000	84	0.2050	25.000
77	61	0.1440	7.000	79	0.1953	17.333
78	83	0.2237	17.333	55	0.1440	4.000
79	84	0.2427	4.333	72	0.2023	56.333
80	56	0.1353	57.333	66	0.1610	13.000
81	85	0.1953	5.333	71	0.1767	6.333
82	55	0.1290	1.000	81	0.1863	54.333
83	51	0.1200	28.000	69	0.1547	34.333
84	81	0.2067	6.333	55	0.1383	5.333
85	62	0.1520	4.000	71	0.1760	36.000
86	52	0.1290	4.000	67	0.1597	6.333
87	67	0.1740	7.000	59	0.1507	12.333
88	78	0.1987	42.333	63	0.1917	6.333

---

---

89	51	0.1373	2.333	69	0.1803	2.333
90	66	0.1493	9.333	80	0.1893	30.333
91	62	0.1500	16.000	55	0.1327	36.333
92	78	0.2007	17.333	60	0.1483	4.333
93	83	0.2113	16.333	71	0.1943	30.333
94	65	0.1647	20.333	77	0.2017	12.333
95	68	0.1697	46.333	81	0.2033	9.333
96	57	0.1443	30.333	70	0.1760	16.000
97	76	0.1957	12.333	71	0.1877	6.333
98	75	0.1937	2.333	85	0.2153	12.333
99	80	0.2153	17.333	50	0.1257	30.333
100	65	0.1630	28.000	51	0.1237	6.333
v1	56	0.1400	400.000	73	0.1857	1.333
v2	81	0.2407	12.333	64	0.1607	8.333
v3	78	0.2320	4.000	63	0.1643	0.333
v4	83	0.2443	5.333	58	0.1450	1.000
v5	68	0.1800	16.000	52	0.1200	4.000

---

### Appendix C. Current & Width of Validation Experiments

Exp. No.	Current 1 (amps)	Width 1 (inches)	Width 2 (inches)	Width 3 (inches)	Current 2 (amps)	Width 3 (inches)	Width 4 (inches)	Width 5 (inches)
v1	56	0.1600	0.1400	0.1200	73	0.1850	0.1870	0.1850
v2	81	0.2440	0.2370	0.2410	64	0.1640	0.1590	0.1590
v3	78	0.2300	0.2320	0.2340	63	0.1640	0.1650	0.1640
v4	83	0.2430	0.2470	0.2430	58	0.1450	0.1460	0.1440
v5	68	0.1800	0.1760	0.1840	52	0.1200	0.1220	0.1180

### Appendix D. Mean & Variance of Width for Validation Experiments

Exp. No.	Current 1 (amps)	Mean Width 1,2,3 (inches)	$\sigma^2$ (inches * (10 <sup>6</sup> ))	Current 2 (amps)	Mean Width 4,5,6 (inches)	$\sigma^2$ (inches* (10 <sup>6</sup> ))
v1	56	0.1400	400.000	73	0.1857	1.333
v2	81	0.2407	12.333	64	0.1607	8.333
v3	78	0.2320	4.000	63	0.1643	0.333
v4	83	0.2443	5.333	58	0.1450	1.000
v5	68	0.1800	16.000	52	0.1200	4.000

## LITERATURE CITED

- ABB. (2017). *IRB 140 Industrial Robot* [Technical Data Sheet pdf]. Retrieved from <http://new.abb.com/products/robotics/industrial-robots/irb-140>
- Alpaydin, E. (2014) *Introduction to machine learning*. Cambridge, MA: The MIT Press.
- Baskaro, A., Tandian, R., Haikal, Edyanto, A., & Saragih, A. (2016). Automatic Tungsten Inert Gas Welding Using Machine Vision and Neural Network on Material SS304. *International Conference on Advanced Computer Science and Information Systems (ICACISIS)*, pp. 427-432.
- CK Worldwide. (2017). *Technical Guide Specifications for TIG Welding*. [pdf document]. Retrieved from <http://www.ckworldwide.com/Form%20116%20%20Technical%20Guide.pdf>
- Dong, H., Huff, S., Cong, M., Zhang, Y., Chen, H. (2016). Backside Weld Bead Shape Modeling using Support Vector Machine (Unpublished report). Texas State University, San Marcos, TX.
- Dong, H., Cong\*, M., Liu, Y., Zhang, Y., Chen, H. (2016) Predicting Characteristic Performance for Arc Welding Process. *IEEE International Conference on Cyber Technology in Automation, Control, and Intelligent Systems (CYBER)*, pp 7-12.
- Dong, H., Cong\*, M., Zhang, Y., Liu, Y., Chen, H. (2017) *IEEE International Conference on Robotics Automation (ICRA)*, pp 1794-1799.
- International Federation of Robotics. (2016). *Industrial Robots 2016* [pdf document]. Retrieved from [https://ifr.org/img/office/Industrial\\_Robots\\_2016\\_Chapter\\_1\\_2.pdf](https://ifr.org/img/office/Industrial_Robots_2016_Chapter_1_2.pdf)

- International Federation of Robotics. (2017). *Executive Summary World Robotics 2017 Industrial Robots*. [pdf document] Retrieved from [https://ifr.org/downloads/press/Executive\\_Summary\\_WR\\_2017\\_Industrial\\_Robots.pdf](https://ifr.org/downloads/press/Executive_Summary_WR_2017_Industrial_Robots.pdf)
- Industrial robot. (2016). *International Organization for Standardization online*. ISO 8373:2012(en). Retrieved from <https://www.iso.org/obp/ui/#iso:std:iso:8373:ed-2:v1:en>
- Kaplan, J. (2016) *Artificial intelligence: What Everyone Needs to Know*. New York, NY: Oxford University Press.
- Keshmiri, S., Zheng, X., Feng, L., Pang, C., & Chew, C. (2015). Application of Deep Neural Network in Estimation of the Weld Bead Parameters. *IEEE/RSJ International Conference on Intelligent Robots and Systems (IROS)*, pp. 3518-3523.
- Lee, Jaeyoung. (2007). *Introduction to Offshore Pipelines & Risers* [pdf document]. Retrieved from <https://www.scribd.com/doc/238620580/Introduction-to-Offshore-Pipelines-Risers-Jaeyoung-Lee>.
- Li, W., Gao, K., Wu, J., Hu, T., Wang, J. (2014). SVM-based information fusion for weld deviation extraction and weld groove state identification in rotating arc narrow gap MAG welding. *The International Journal of Advanced Manufacturing Technology*, vol. 74, pp. 1355-1364.
- Liu, Y.K., Zhang, W.J., & Zhang, Y. M. (2013). Neuro-fuzzy based human intelligence modeling and robust control in Gas Tungsten Arc Welding Process. *American Control Conference (ACC)*, pp. 5631-5636.

- Liu, Y.K., & Zhang, Y.M. (2014). Model-Based Predictive Control of Weld Penetration in Gas Tungsten Arc Welding. *IEEE Transactions on Control Systems Technology*, vol. 22, no. 3, pp. 955-966.
- Liu, Y.K., Zhang, W.J., & Zhang, Y.M. (2015). Dynamic Neuro-Fuzzy-Based Human Intelligence Modeling and Control in GTAW. *IEEE Transactions on Automation Science and Engineering*, vol. 12, no. 1, pp. 324-335.
- Patel, R. B., & Patel, N. S. (2014). A Review of Parametric Optimization of Tig Welding. *International Journal of Computational Engineering Research*, 04, pp 27-31.
- Rasmussen, C. E., Nickisch, H. (2017). Code from the Rasmussen and Williams: Gaussian Process for Machine Learning book [Software]. Available from <http://www.gaussianprocess.org/gpml/code/matlab/doc/index.html>
- Russel, S. J., Norvig, P. (1995) *Artificial Intelligence: A Modern Approach*. Upper Saddle River, NJ: Prentice Hall Publishing.
- Snelson, E. (2006) *Tutorial: Gaussian process models for machine learning* [pdf document]. Retrieved from <http://mlg.eng.cam.ac.uk/tutorials/06/es.pdf>
- Sterling, D., Sterling, T., Zhang, Y., Chen, H. (2015). Welding Parameter Optimization Based on Process Regression Bayesian Optimization Algorithm. *IEEE International Conference on Automation Science and Engineering (CASE)*, pp. 1490-1496.
- Vinas, J., Cabrera, R., Juarez, I. (2016). On-line learning of welding bead geometry in industrial robots. *International Journal of Advanced Manufacturing Technology*, vol. 83, pp. 217-231.



- Wallen, Johanna. (2008, May 8). The history of the industrial robot. *Technical report from Automatic Control at Linkopings universitet*, LiTH-ISY-R-2853, 6-10.
- Retrieved from
- <http://liu.divaportal.org/smash/get/diva2:316930/FULLTEXT01.pdf>
- Wang , S., Chaovalitwongse, W., & Babuska, R (2012). Machine learning algorithms in bipedal robot control. *IEEE Transactions on Systems Man and Cybernetics Part C: Applications and Reviews*, vol. 42, no. 5, pp. 728-743.
- Wang, X., Li, R. (2014). Intelligent modelling of back-side weld bead geometry using weld pool surface characteristic parameters. *Journal of Intelligent Manufacturing*, vol. 25, no. 6, pp. 1301-1313.
- Wang, X., Liu, Y.K., Zhang, W.J., & Zhang, Y. M. (2012). Estimation of weld penetration using parameterized three-dimensional weld pool surface in gas tungsten arc welding. *IEEE International Symposium on Industrial Electronics (ISIE2012)*, pp. 835-840.
- Zhang, W.J., & Zhang, Y. M. (2012). Modeling of Human Welder Response to 3D Weld Pool Surface: Part I-Principles. *Welding Journal* 91(11): 310-s to 318-s.